

Focal structural variants revealed by whole genome sequencing disrupt the histone demethylase KDM4C in B-cell lymphomas

Cristina López,^{1,2*} Nikolai Schleussner,^{3,4*} Stephan H. Bernhart,^{5,6,7} Kortine Kleinheinz,⁸ Stephanie Sungalee,⁹ Henrike L. Sczakiel,^{3,4} Helene Kretzmer,^{5,6,7,10} Umut H. Toprak,^{11,12,13} Selina Glaser,¹ Rabea Wagener,^{1,2} Ole Ammerpohl,^{1,2} Susanne Bens,^{1,2} Maciej Giefing,^{2,14} Juan C. González Sánchez,¹⁵ Gordana Apic,¹⁵ Daniel Hübschmann,^{16,17,18} Martin Janz,^{3,4} Markus Kreuz,¹⁹ Anja Mottok,¹ Judith M. Müller,²⁰ Julian Seufert,¹¹ Steve Hoffmann,^{5,6,7,21} Jan O. Korbel,⁹ Robert B. Russell,¹⁵ Roland Schüle,^{20,22} Lorenz Trümper,²³ Wolfram Klapper,²⁴ Bernhard Radlwimmer,²⁵ Peter Lichter,²⁵ Ralf Küppers,²⁶ Matthias Schlesner,^{11,27} Stephan Mathas^{3,4#} and Reiner Siebert^{1,2#} and members of the ICGC MMML-Seq Consortium

¹Institute of Human Genetics, Ulm University and Ulm University Medical Center, Ulm, Germany;

²Institute of Human Genetics, Christian-Albrechts-University, Kiel, Germany; ³Max-Delbrück-Center for Molecular Medicine in the Helmholtz Association (MDC), Berlin, Germany;

⁴Hematology, Oncology and Tumor Immunology, Charité - Universitätsmedizin Berlin, Berlin, Germany, and Experimental and Clinical Research Center, a joint cooperation between the MDC and the Charité, Berlin, Germany;

⁵Interdisciplinary Center for Bioinformatics, University of Leipzig, Leipzig, Germany; ⁶Bioinformatics Group, Department of Computer, University of Leipzig, Leipzig, Germany;

⁷Transcriptome Bioinformatics, LIFE Research Center for Civilization Diseases, University of Leipzig, Leipzig, Germany; ⁸Department for Bioinformatics and Functional Genomics, Institute of Pharmacy and Molecular Biotechnology and Bioquant, University of Heidelberg, Heidelberg, Germany;

⁹EMBL Heidelberg, Genome Biology Unit, Heidelberg, , Germany; ¹⁰Department of Genome Regulation, Max Planck Institute for Molecular Genetics, Berlin, Germany;

¹¹Bioinformatics and Omics Data Analytics (B240), German Cancer Research Center (DKFZ), Heidelberg, Germany; ¹²Faculty of Biosciences, Heidelberg University, Heidelberg, Germany;

¹³Hopp-Children's Cancer Center at the NCT Heidelberg (KITZ), Division of Neuroblastoma Genomics (B087), German Cancer Research Center (DKFZ), Heidelberg, Germany;

¹⁴Institute of Human Genetics, Polish Academy of Sciences, Poznan, Poland; ¹⁵BioQuant and Biochemie Zentrum Heidelberg (BZH), Heidelberg University, Heidelberg, Germany;

¹⁶German Cancer Consortium (DKTK), Heidelberg, Germany; ¹⁷Heidelberg Institute of Stem Cell Technology and Experimental Medicine (HI-STEM), Heidelberg, Germany;

¹⁸Computational Oncology, Molecular Precision Oncology Program, National Center for Tumor Diseases (NCT), German Cancer Research Center (DKFZ) and German Cancer Consortium (DKTK), Heidelberg, Germany;

¹⁹Institute for Medical Informatics Statistics and Epidemiology, Leipzig, Germany; ²⁰Klinik für Urologie und Zentrale Klinische Forschung, Klinikum der Albert-Ludwigs-Universität Freiburg, Freiburg, Germany;

²¹Leibniz Institute on Ageing-Fritz Lipmann Institute (FLI), Computational Biology, Jena, Germany; ²²BIOSS Centre of Biological Signalling Studies, Albert-Ludwigs-Universität Freiburg, Freiburg, Germany;

²³Department of Hematology and Oncology, Georg-August-University of Göttingen, Göttingen, Germany; ²⁴Hematopathology Section, Christian-Albrechts-University, Kiel, Germany;

²⁵Division of Molecular Genetics, German Cancer Research Center (DKFZ), Heidelberg, Germany; ²⁶Institute of Cell Biology (Cancer Research), University of Duisburg-Essen, Essen, Germany, and German Cancer Consortium (DKTK) and ²⁷Biomedical Informatics, Data Mining and Data Analytics, Augsburg University, Augsburg, Germany

²⁸Department of Hematology and Oncology, Georg-August-University of Göttingen, Göttingen, Germany; ²⁹Hematopathology Section, Christian-Albrechts-University, Kiel, Germany;

³⁰Division of Molecular Genetics, German Cancer Research Center (DKFZ), Heidelberg, Germany; ³¹Institute of Cell Biology (Cancer Research), University of Duisburg-Essen, Essen, Germany, and German Cancer Consortium (DKTK) and ³²Biomedical Informatics, Data Mining and Data Analytics, Augsburg University, Augsburg, Germany

*CL and NS contributed equally as co-first authors.

#SM and RS contributed equally as co-senior authors.

Abstract

Histone methylation-modifiers, such as *EZH2* and *KMT2D*, are recurrently altered in B-cell lymphomas. To comprehensively describe the landscape of alterations affecting genes encoding histone methylation-modifiers in lymphomagenesis we investigated whole genome and transcriptome data of 186 mature B-cell lymphomas sequenced in the ICGC MMML-Seq project. Besides confirming common alterations of *KMT2D* (47% of cases), *EZH2* (17%), *SETD1B* (5%), *PRDM9* (4%), *KMT2C* (4%), and *SETD2* (4%), also identified by prior exome or RNA-sequencing studies, we here found

Correspondence:

R. Siebert
reiner.siebert@uni-ulm.de

S. Mathas
stephan.mathas@charite.de

Received: September 13, 2021.

Accepted: March 18, 2022.

Prepublished: April 28, 2022.

<https://doi.org/10.3324/haematol.2021.280005>

©2023 Ferrata Storti Foundation

Published under a CC BY-NC license



recurrent alterations to *KDM4C* in chromosome 9p24, encoding a histone demethylase. Focal structural variation was the main mechanism of *KDM4C* alterations, and was independent from 9p24 amplification. We also identified *KDM4C* alterations in lymphoma cell lines including a focal homozygous deletion in a classical Hodgkin lymphoma cell line. By integrating RNA-sequencing and genome sequencing data we predict that *KDM4C* structural variants result in loss-of-function. By functional reconstitution studies in cell lines, we provide evidence that *KDM4C* can act as a tumor suppressor. Thus, we show that identification of structural variants in whole genome sequencing data adds to the comprehensive description of the mutational landscape of lymphomas and, moreover, establish *KDM4C* as a putative tumor suppressive gene recurrently altered in subsets of B-cell derived lymphomas.

Introduction

The majority of mature B-cell malignancies originates from the germinal center (GC) B cell or the post-GC stage.¹ Historically, Hodgkin lymphoma (HL) and non-Hodgkin lymphomas (NHL) are distinguished. The neoplastic Hodgkin-/Reed-Sternberg cells in classical HL (cHL) are supposed to be derived from pre-apoptotic GC B cell.¹ The most prevalent types of GC-derived NHL are diffuse large B-cell lymphoma (DLBCL) and follicular lymphoma (FL).² DLBCL is an aggressive disease, composed of various subtypes including the gene expression-based GC B-cell like (GCB) and activated B-cell like (ABC) types,^{2,3} or recently genomically defined groups.^{4–10} FL is a more indolent disease which occasionally transforms into DLBCL.¹¹

The immanent genomic instability of B cells during the GC reaction, which is required for the formation of antibody diversity, is assumed to be causative for malignant transformation of GC or post-GC B cells.¹² The GC reaction requires a tightly controlled balance between proliferation and growth arrest, and between full cellular activation or a rather resting stage. Epigenetic modifiers are key regulators of these “on-off” stages.¹² In line, they are common targets of genomic alterations in GC-derived B-cell lymphomas,¹¹ including the genes encoding the histone methyltransferases *KMT2D*, *KDMT2C* and *EZH2*, the histone acetyltransferases *CREBBP* and *EP300*,^{6,13–15} and the chromatin remodelers including members of the SWI/SNF complex.¹⁶ A series of recent studies investigated genomic alteration frequencies in oncogenic drivers including epigenetic modifiers in huge series of patients with DLBCL, but also FL. These studies, investigating in total more than 1,800 DLBCL (Chapuy *et al.*, n=304;⁵ Schmitz *et al.*, n=574;⁶ Reddy *et al.*, n= 1,001¹⁴), found aberrations in *KMT2D* (24–31%), *CREBBP* (11–17%), and *EP300* (6–8%).^{5,6,14} Consequently, alterations in these histone modifiers contribute to the definition of genetic subgroups of DLBCL, such as cluster 3 in Chapuy *et al.*,⁵ or the EZB group in Schmitz *et al.*⁶ and Wright *et al.*,⁴ the BCL2 group in Lacy *et al.*⁸ and the EZH2 group in Hübschmann *et al.*⁷ Most of these studies characterized the genomic alteration landscape predominantly by exome or otherwise targeted sequencing, in part combined with transcriptome sequencing.¹⁰ Methodically, however, although this approach detects single nucleotide variants

(SNV), small insertions and deletions (indels) and gross imbalances, it has an inherent weakness in the detection of some structural variants such as intragenic deletions, chromosomal translocations, and inversions.¹⁷

To overcome this shortcoming, we here mined data from whole genome sequencing (WGS) of 186 GC-derived B-cell lymphomas and 183 corresponding germline DNA samples generated by us in the framework of the International Cancer Genome Consortium (ICGC) Molecular Mechanisms in Malignant Lymphoma by Sequencing (MMML-Seq) project (<https://dcc.icgc.org>).^{7,18–20} Given the increasing pathogenic, diagnostic and therapeutic importance of altered histone methylation in B-cell lymphomas,^{11,13,21} we focused here on 79 genes encoding histone methylation modifiers.

Methods

Whole genome and transcriptome sequencing data

We mined WGS data and available RNA-sequencing data of 186 GC-derived B-cell lymphomas from the ICGC MMML-Seq network⁷ (*Online Supplementary Methods*). The ICGC MMML-Seq study has been approved by the Institutional Review Board of the Medical Faculties of the University of Kiel (A150/10) and Ulm (349/11), and of the recruiting centers. Methods and procedures used in the ICGC MMML-Seq project have been detailed in various publications^{7,18,20,22,23} of the network. Sequencing data are available from the European Genome-phenome Archive (EGA) (accession number EGAS00001002199). The genomic status of 79 genes encoding histone methylation modifiers (selected based on <http://crdd.osdd.net/raghava/dbem/index.php>, accessed 01/03/2018; *Online Supplementary Table S1*) was investigated.

Cell lines and cell line data

Nineteen B- and T-cell NHL and four cHL-derived cell lines were used in the study (*Online Supplementary Table S2*). The identity of the cell lines used was confirmed by short tandem repeat analysis using the StemElite ID System (Promega). Copy number data²⁴ and/or exome data²⁵ from previously published studies on the four cHL cell lines herein analyzed and two additional cHL cell lines were included as well as previously reported WGS data from the cHL cell line L1236.²⁶

Bioinformatics analyses

The computational approaches for the analysis of WGS and transcriptome data were recently described²⁰ (*Online Supplementary Materials and Methods*). Briefly, WGS data were analyzed using the DKFZ core variant calling workflows of the ICGC Pan-Cancer Analysis of Whole Genomes (PCAWG) project. Allele-specific copy-number alterations were analyzed using ACE-seq and structural variants were called using the SOPHIA algorithm²⁰ and DELLY v0.5.9.^{27,28} To determine the incidence of structural variants in the PCWAG, filtered structural variant calls were generated by SOPHIA for the PCAWG cohorts processed with the same tools and settings as with the lymphoma cohort used in this study. Transcriptome data were mapped with segemehl 0.2.0.²⁹ Gene expression values were counted by the RNAcounter 1.5.2, using the “--nh” option and counting only exonic reads (-t exon).

Mechismo (<http://mechismo.russelllab.org/>) was used to predict the potential effect of structural variants and SNV detected by WGS.

Verification of *KDM4C* alterations by polymerase chain reaction-based Sanger sequencing and fluorescence *in situ* hybridization

Verification analyses on a DNA level included polymerase chain reaction (PCR) amplification with subsequent Sanger sequencing and fluorescent *in situ* hybridization (FISH) (*Online Supplementary Materials and Methods*). Alternative *KDM4C* fusion transcripts were validated using specific primers to amplify breakpoint fusion sequences from tumor RNA-derived cDNA (*Online Supplementary Materials and Methods*) and Sanger sequencing. Verifications using FISH were done using two home-made FISH-probes, i.e., using locus-specific and break-apart *KDM4C* probes (*Online Supplementary Material and Methods*). Digital image acquisition, processing, and evaluation of FISH assays were performed using ISIS digital image analysis version 5.0 (MetaSystems, Altusheim, Germany). The same FISH approaches were used to evaluate the genomic status of *KDM4C* in lymphoma cell lines.

Functional analyses

For functional analyses, the respective cells were transfected with doxycycline-inducible *KDM4C* expression constructs or transduced with *KDM4C*-encoding lentiviruses (*Online Supplementary Materials and Methods*). For generation of *KDM4C*-inducible cells, cells were electroporated in OPTI-MEM I using Gene-Pulser II (Bio-Rad). Twenty-four hours after transfection, hygromycin B (Sigma-Aldrich, Taufkirchen, Germany) was added. After 21–28 days of culture in the presence of hygromycin B, cells were suitable for functional assays. Where indicated, green fluorescent protein-positive (GFP⁺) cells were enriched 72 h after doxycycline-induction using a FACS Aria. Production of lentivi-

ruses and lentiviral transduction of cells was performed as described previously³¹ (*Online Supplementary Materials and Methods*). *KDM4C* protein expression was assessed by western blot, and immunohistochemistry using a rabbit polyclonal anti-*KDM4C* antibody raised against amino acids 1007–1056.

Results

Aberrations in genes encoding histone methylation modifiers in the ICGC MMML-Seq cohort determined by whole genome sequencing

We analyzed WGS data of 186 GC-derived B-cell lymphomas⁷ for somatic aberrations potentially perturbing gene function, including SNV, indels, structural variants and focal copy number aberrations affecting at least two cases in 79 genes encoding histone methylation modifiers. The genes most commonly affected were *KMT2D* (47% of cases), *EZH2* (17%), *SETD1B* (5%), *KDM4C* (4%), *PRDM9* (4%), *KMT2C* (4%), and *SETD2* (4%) (Figure 1A).

The genes identified and their frequency of alteration in our cohort are grossly in line with previous analyses of DLBCL cohorts.^{5,6,14} However, alterations of *KDM4C* have not been emphasized as a recurrent finding in previous whole exome studies of GC B-cell lymphomas. *KDM4C* (also called *JMJD2C*) encodes a member of the Jumonji family of demethylases, which activate genes by removing methyl groups from histones H3K9 and H3K36.^{32,33}

Genomic alterations affecting the *KDM4C* gene locus

We detected aberrations of *KDM4C* in 7/186 (3.7%) of all cases, and in 4/75 (5.3%) of *bona fide* DLBCL. In detail, we detected a total of seven focal aberrations in *KDM4C*, including four heterozygous deletions, one duplication, one translocation and one non-synonymous SNV each, affecting seven patients (Figure 1B; *Online Supplementary Table S2*). The minimum read number supporting *KDM4C* alterations was four reads. The cancer cell fraction or the proportion of cancer cells with a *KDM4C* alteration among all cancer cells suggests that these alterations are clonal in GC B-cell lymphomas (*Online Supplementary Table S2*). We verified all *KDM4C* aberrations by FISH using homemade FISH assays and/or PCR and Sanger sequencing (*Online Supplementary Table S2*).

Pathological and genetic features of the lymphomas with *KDM4C* gene alterations

The cases displaying *KDM4C* alterations included four of 75 DLBCL (5.3%), one of 17 FL-DLBCL (5.9%), one of four (25%) large B-cell lymphomas with *IRF4*-rearrangement, and the one primary mediastinal B-cell lymphoma (Table 1). We explored whether cases with *KDM4C* aberrations diagnosed as DLBCL (n=4) cluster in a specific genomic subgroup ac-

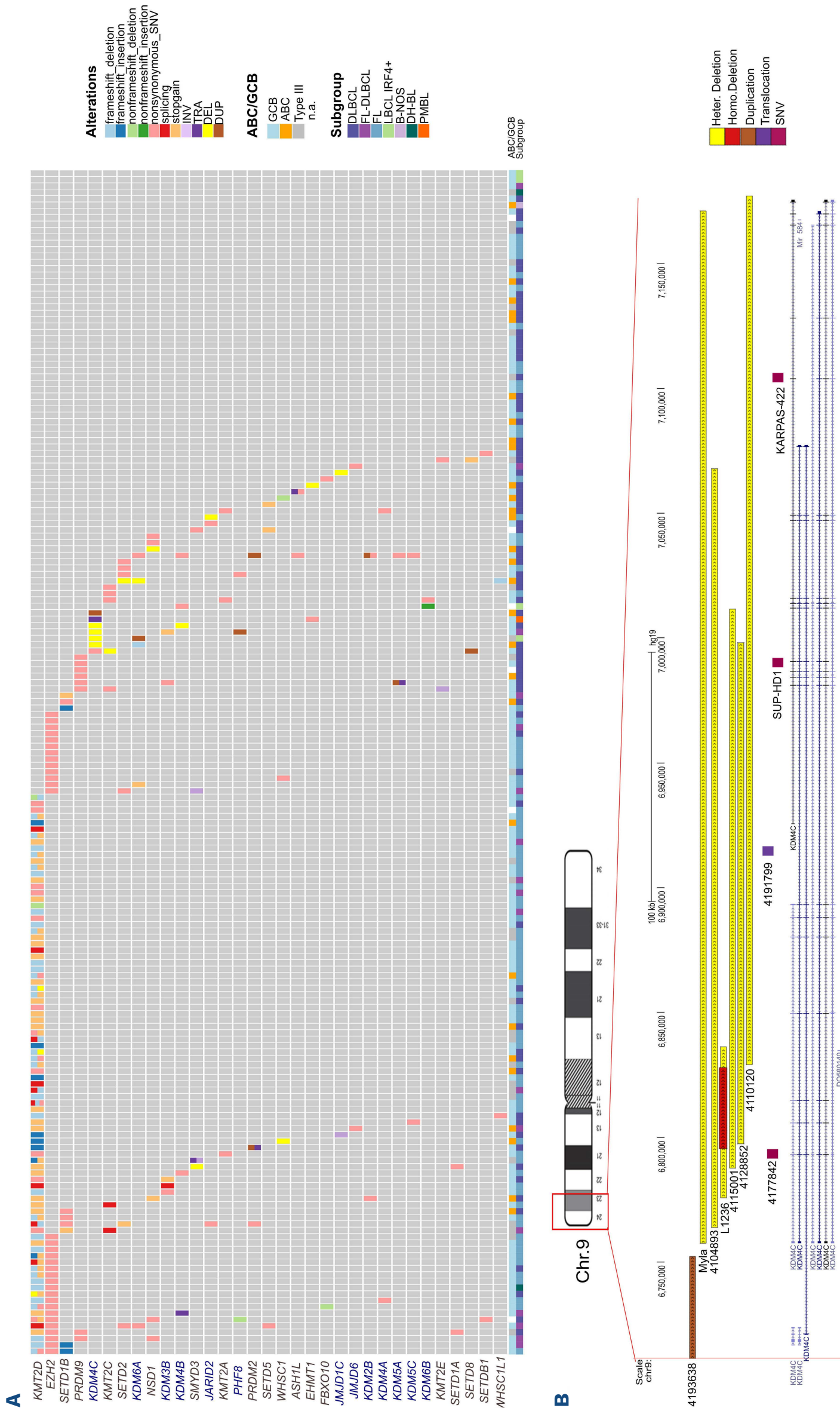


Figure 1. Genomic aberrations of genes encoding histone methyltransferases in germinal center-derived B-cell lymphomas. (A) Genes encoding histone methyltransferases affected by single nucleotide variants, structural variants, focal copy number aberrations, and indels in at least two of the studied germinal center-derived B-cell lymphomas. The events are shown independently of the transcript isoform affected. Genes encoding histone methyltransferases are named in gray, genes encoding demethylases in blue. Categorization according to diagnosis and cell-of-origin classification is shown. The respective type of variant is indicated by color. Only focal aberrations are displayed. (B) UCSC genome browser track (accessed 03.02.2021) displaying the *KDM4C* genomic aberrations detected in primary lymphomas and lymphoma cell lines. The type of variant is indicated by color and each focal aberration in a separate line. Note, the size of the squares showing the single nucleotide variants and translocations is not representative of the real size of the genomic aberration to improve the visualization. The heterozygous deletions and the homozygous deletion are labeled in yellow and red, respectively. Duplication is indicated by a brown color and the translocation in purple. The breakpoints of the genomic aberrations are annotated based on hg19 and the *KDM4C* transcripts displayed as provided by UCSC Genes track. Note, that the L1236 cell line shows homozygously and heterozygously deleted regions. INV: inversion; TRA: translocation; DEL: deletion; DUP: duplication; ABC: activated B-cell; n.a.: not available; DLBCL: diffuse large B-cell lymphoma; FL: follicular lymphoma; LBCL: large B-cell lymphoma; B-NOS: B-cell not otherwise specified; DH-BL: Double hit-Burkitt lymphoma; PMBL: primary mediastinal B-cell lymphoma; Heter: heterozygous, Homo: homozygous; SNV: single nucleotide variation. Note, the display of *KDM4C* deletion in My-La is an estimation, an exact breakpoint could not be determined by fluorescent *in situ* hybridization.

ording to the non-negative matrix factorization (NMF) clustering described previously by our group,⁷ which resembles features of genetic DLBCL subgroups previously also described by others^{4,5} (Table 1). Using the described four-cluster classifier limited to DLBCL cases, we identified two MYD88-like and two TP53-like cases. Using the nine-subcluster classifier established for the whole ICGC MMML-Seq FL and DLBCL cohort, we assigned two cases to the PIM1-like cluster, two cases to the PAX5-like cluster and one case to the MYD88-like cluster (2 cases other than DLBCL or FL not included in the previous NMF analyses, i.e. 1 primary mediastinal B-cell lymphoma and 1 *IRF4* rearrangement-positive large B-cell lymphoma). Furthermore, we explored the distribution of *KDM4C*-altered cases diagnosed as DLBCL (n=4) among transcriptional subgroups based on the cell-of-origin signature. Two cases were classified as GCB-like and two cases as ABC-like lymphomas. Thereafter, we extended the analysis to the whole cohort and we observed that four of seven cases with *KDM4C* aberrations displayed a GCB signature and two of seven cases an ABC signature (1 case assigned to Type III/unclassified). Overall, *KDM4C* aberrations were not significantly enriched in any specific genetic or transcriptional subtype of the analyzed lymphomas.

In addition, we explored whether *KDM4C* aberrations were associated with the 9p24.1 amplification, as described previously.³⁴ In five out of seven cases with *KDM4C* focal aberrations, we did not detect 9p24.1 gain (*Online Supplementary Figures S1* and *S2*). This indicates that the vast majority of focal *KDM4C* aberrations occurred independently of 9p24 amplifications. We also explored aneuploidy of chromosome 9 and the general genomic ploidy of the *KDM4C*-altered cases. We did not observe a significant increase of chromosome 9 gains (*Online Supplementary Figure S2*) or polyploid genome contents (*Online Supplementary Figure S3*) in cases with *KDM4C* aberrations as compared to cases without such aberrations. Furthermore, we investigated whether the *KDM4C* aberrations occurred preferentially in lymphomas with highly rearranged genomes that were predisposed to carry these events by chance. We identified a mean of 73.85 structural variants per case (range, 34–144) in lymphomas with *KDM4C* aberration compared to a mean of 83.24 structural variants per case (range, 5–1696) in lymphomas lacking *KDM4C* aberrations. The mean number of structural variants was not significantly different between the two groups of patients (Wilcoxon test, $P=0.125$) (*Online Supplementary Figure S4*).

***KDM4C* alterations as potential tumor drivers**

KDM4C is located in a early replicating genomic region in B cells (at the border of a late replicating region) based on the ENCODE Repli-seq data from different lymphoblastoid cell lines³⁵ (*Online Supplementary Figure S5*). This fact sug-

gests that mutation of the gene is not a passenger effect caused by late replication. Furthermore, we examined

Table 1. Characteristics and biological features of the cohort. Overview of the age, sex, and lymphoma subtype distribution of the cohort and of *KDM4C*-affected cases.

	Whole cohort (N=186)	<i>KDM4C</i> focal aberrations (N=7)
Median age at diagnosis, years (range)	62.5 (16-89)	57 (16-75)
Male, N (%)	84 (45)	3 (42.9)
Diagnostics, N (%)		
DLBCL	75 (40.3)	4 (57)
FL	86 (46.2)	0
FL-DLBCL	17 (9.1)	1 (14.3)
LBCL-with <i>IRF4</i> breaks	4 (2.2)	1 (14.3)
B-NOS	1 (0.55)	0
DH-BL	2 (1.1)	0
PMBL	1 (0.55)	1 (14.3)
Cell of origin, N (%)		
GCB	124/182 (68.1)	4 (57.1)
ABC	29/182 (15.9)	2 (28.6)
Type III	29/182 (15.9)	1 (14.3)
Hallmark events, N (%)		
<i>MYC</i> breaks	18/185 (9.7)	0
<i>BCL2</i> breaks	106/185 (57.3)	2 (28.6)
<i>BCL6</i> breaks	51 (27.4)	2 (28.6)
NMF subclusters (4 categories, only DLBCL) ⁷ , N (%)		
BCL2-like	10/72 (13.9)	0/4 (0)
BCL6-like	17/72 (23.6)	0/4 (0)
MYD88-like	26/72 (36.1)	2/4 (50)
TP53-like	19/72 (26.4)	2/4 (50)
NMF subclusters (9 categories) ⁷ , N (%)		
B2M like	13/179 (7.3)	0/5 (0)
BCL2-like	35/179 (19.5)	0/5 (0)
BCL6-like	23/179 (12.8)	0/5 (0)
MYD88-like	17/179 (9.5)	1/5 (20)
PAX5-like	19/179 (10.6)	2/5 (40)
PIM1-like	18/179 (10)	2/5 (40)
TP53-like	19/179 (10.6)	0/5 (0)
CSMD1-like	20/179 (11.2)	0/5 (0)
SOCS1-like	15/179 (8.4)	0/5 (0)

Cell of origin based on gene expression classification. N: number; DLBCL: diffuse large B-cell lymphoma; FL: follicular lymphoma; LBCL: large B-cell lymphoma; B-NOS: B-cell lymphoma not otherwise specified; PMBL: primary mediastinal B-cell lymphoma; GCB: germinal center B-cell like; ABC: activated B-cell like; NMF: non-negative matrix factorization.

whether the breakpoints were located in the RGYW/WRCY motif typically associated with the activation-induced cytidine deaminase (AID) enzyme³⁶ that is active in GC B cells. However, none of the breakpoints directly hits these motifs. These facts suggest that mutation of the *KDM4C* gene in lymphoma is not a bystander effect caused by late replication or aberrant somatic hypermutation.

Next we analyzed the incidence of structural variants affecting the *KDM4C* locus in the 45 tumor datasets with WGS available included in the PCWAG.¹⁹ We identified 14 cohorts with an incidence of *KDM4C* alterations equal to or higher than that reported herein (*Online Supplementary Figure S6*). Importantly, the cohort with the highest incidence of structural variant breakpoints affecting *KDM4C* was the DLBCL-US cohort, corroborating our findings and highlighting the relevance of *KDM4C* alterations in this subgroup of B-cell lymphomas. Other types of cancers harboring structural variants in *KDM4C* were renal, head and neck, ovarian, hepatocarcinoma, esophageal, bladder, prostate, osteosarcoma, and gastric cancer, suggesting that *KDM4C* alterations might not be restricted to lymphomas. A role of *KDM4C* in these tumors has been discussed previously.³⁷⁻⁴⁴

Molecular consequence of *KDM4C* aberrations

The *KDM4C* protein consists of an N-terminal catalytic domain (JmjN and JmjC) followed by three zinc-fingers (PHD or C2H2) and two C-terminal Tudor domains.⁴⁵ By

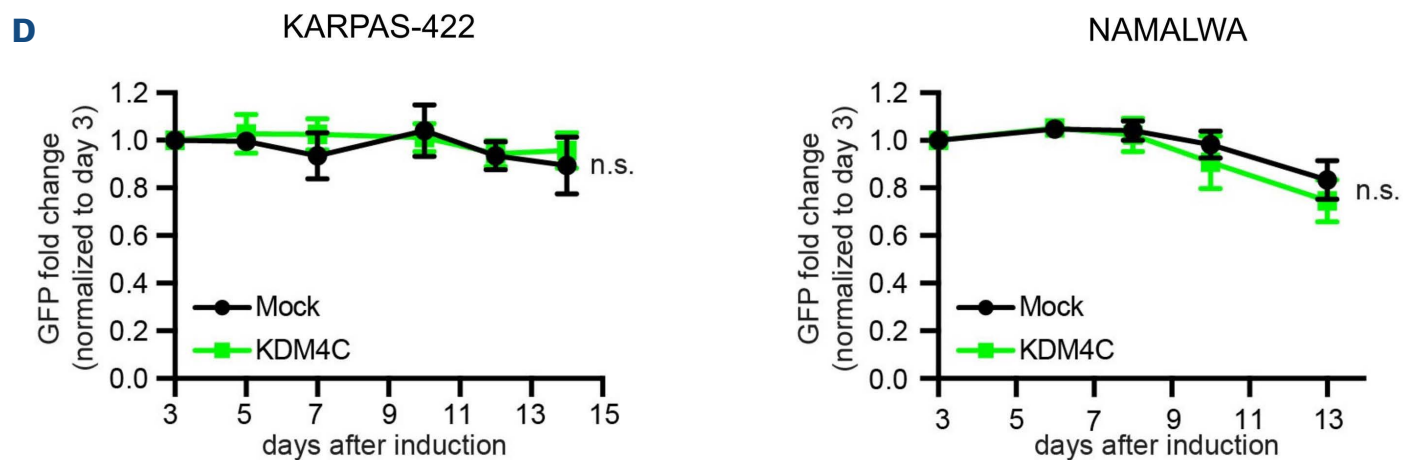
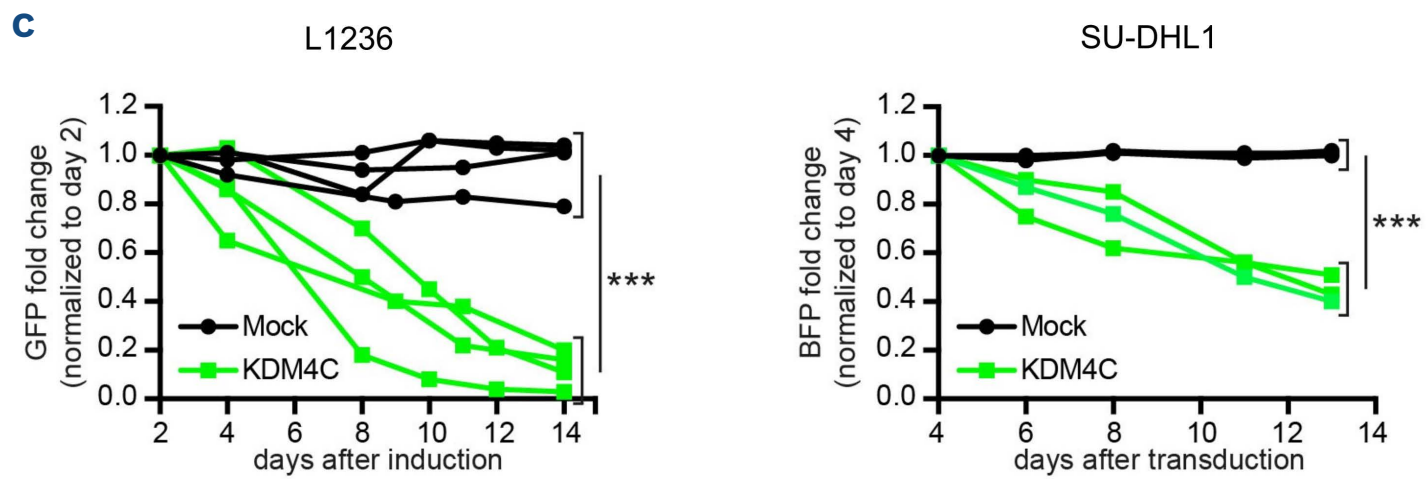
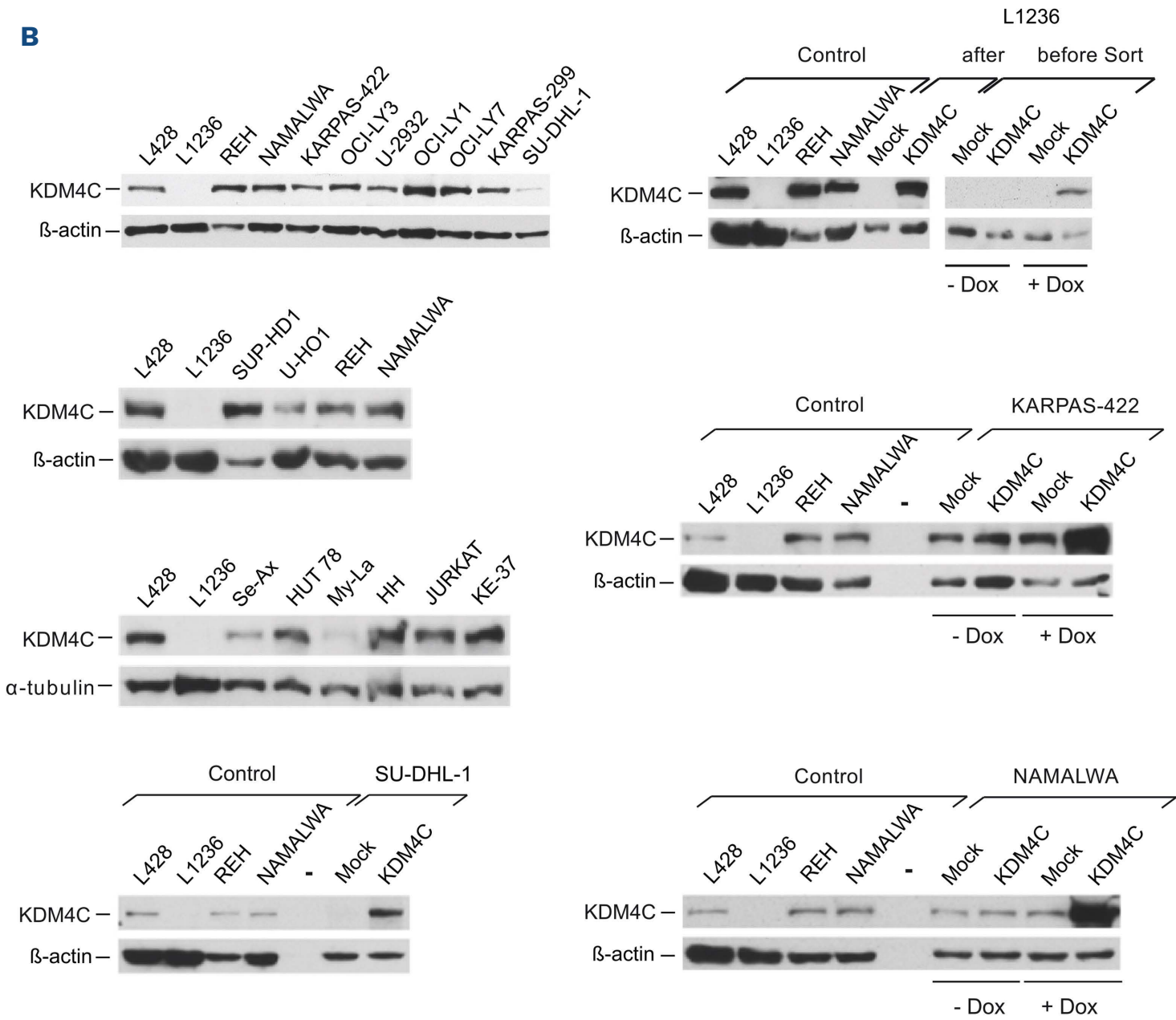
integrating RNA-sequencing and WGS data in the six cases with focal structural variants and available transcriptome data (4 focal heterozygous deletions, 1 translocation, and 1 duplication), we detected alternative *KDM4C* transcripts in five of them, which were verified by reverse transcriptase PCR and sequencing (*Online Supplementary Table S2*). *In silico* analyses using Mechismo (<http://mechismo.russelllab.org/>) predicted that these alternative transcripts would result in altered proteins lacking the catalytic or recognition (epigenetic readers) domains (Figure 2A). *In silico* modeling of the non-synonymous somatic SNV (c.G80A, p.R27Q) detected in case 4177842, which lies in the JmjN domain, suggests a possible functional consequence on protein function (*Online Supplementary Figure S1*).

Lack of epigenetic alterations at the *KDM4C* locus due to *KDM4C* mutation

As to the recently proposed role of a circular RNA (circRNA) derived from the *KDM4C* locus (circ*KDM4C*) in repression of proliferation and metastasis in breast cancer,⁴⁶ we also explored expression of circ*KDM4C* in the RNA-sequencing data of our cohort. We identified circ*KDM4C* expression in three cases (3/180, 1.7%), but none of them showed an alteration of the *KDM4C* locus (*data not shown*). In addition, we investigated the epigenetic architecture at the *KDM4C* locus by mining previously published whole genome bisulfite sequencing and array-



Continued on following page.



Continued on following page.

Figure 2. Potential tumor suppressive role of the *KDM4C* protein. (A) Predicted *KDM4C* protein alterations associated with genomic and transcriptomic changes. Top panel: structure of the *KDM4C* protein (Uniprot: Q9H3R0) with highlighted positions of the two N-terminal JmjN and JmjC catalytic domains, the PHD zinc finger domains, and the two C-terminal Tudor recognition domains. Boxes highlight the predicted residual protein structure (if translated) in lymphoma cases and cell lines with somatic *KDM4C* variants. In case 4177842, the single nucleotide variant (SNV) affects the JmjN domain. In cases 4191799 and 4110120 the regulatory/recognition region is affected, in cases 41074893, 4128852 and 4115001 the catalytic domains are affected. The predicted protein in KARPAS-422 affects the regulatory region; in L1236 the predicted protein abrogates the catalytic domain JmjC, and the regulatory/recognition region, and consequently generates a non-functional protein; in SUP-HD1 the regulatory/recognition domains are predicted to be lost by the truncating SNV. See the extended legend to Figure 2SA in the *Online Supplementary Material* for more detail. (B) Immunoblotting of *KDM4C* protein. Left column, upper three panels, *KDM4C* protein expression in whole cell extracts of various human leukemia/lymphoma-derived cell lines, as indicated. β -actin or α -tubulin are shown as controls. Note that L1236 cells completely lack *KDM4C* protein expression, and *KDM4C* expression in SU-DHL-1, My-La and Se-Ax cells is strongly reduced. Upper right panel, *KDM4C* immunoblotting of L1236 cells before and after transfection with a doxycycline (Dox)-inducible *KDM4C*-expression vector or respective control (Mock) construct, before (left) and after (right) enrichment of Dox-induced GFP⁺ cells. β -actin is shown as a control. Right column, center and bottom, immunoblotting of *KDM4C* of KARPAS-422 and NAMALWA after transfection with Dox-inducible *KDM4C* or control (Mock) construct, without and after addition of Dox. β -actin is shown as a control. Left column bottom, immunoblotting of *KDM4C* of SU-DHL-1 cells after lentiviral transduction with *KDM4C* expression or respective control (Mock) construct. Note, that L428, L1236, REH and NAMALWA extracts were included as positive and negative controls. (C, D) Reconstitution of *KDM4C* results in loss of cells re-expressing *KDM4C* in L1236 and SU-DHL-1 in which endogenous expression of the protein is absent and reduced, respectively, but not in those with robust endogenous *KDM4C* expression (KARPAS-422, NAMALWA). (C) Left, L1236 cells were transfected with Dox-inducible *KDM4C*-expression or respective control (Mock) construct. GFP expression is driven in parallel to *KDM4C* by a bidirectional promoter. GFP⁺ cells were enriched by flow cytometry 48 h after addition of Dox and, thereafter, the percentage of GFP⁺ cells was monitored over time by flow cytometry. The percentages of *KDM4C*- or Mock-transfected GFP⁺ cells normalized to the percentage of GFP⁺ cells at day 2 after Dox-induction and enrichment of GFP⁺ cells is shown. Right, SU-DHL-1 cells were lentivirally transduced with *KDM4C*, and the percentage of *KDM4C*, EBFP⁺ cells over time was determined as described for L1236 cells. (D) KARPAS-422 (left) and NAMALWA (right) cells were treated and monitored as described in (C) for L1236, with the difference that due to high transfection rates for both cell lines no enrichment of GFP⁺ cells was required.

based DNA methylation, as well as chromatin state data.²² The promoter and transcription start site region showed strong hypomethylation in all subtypes of lymphomas and B-cell controls (*Online Supplementary Figure S7*). We did not observe any differential DNA methylation with regard to expression or alteration of the *KDM4C* locus with the notable exception of CpG cg13880654 associated with an intronic enhancer site which was hypermethylated in the majority of lymphoma cell lines other than Burkitt lymphoma cell lines. Together, the pattern of alterations strongly suggests *KDM4C* protein loss-of-function as a common effect of the *KDM4C* gene aberrations (Figure 2A, *Online Supplementary Figure S1*), indicative of a tumor suppressor function of *KDM4C* protein.

Transcriptional analyses

Using the RNA-sequencing data, we investigated *KDM4C* transcript expression in the seven cases with *KDM4C* alterations compared to 173 GC B-cell lymphomas without *KDM4C* aberrations. To reduce confounders, we performed these analyses for each lymphoma subtype separately. No statistically significant difference in *KDM4C* transcript expression was observed between samples with altered as compared to wildtype *KDM4C* in FL-DLBCL ($P=0.4706$), in DLBCL ($P=0.2095$), or in large B-cell lymphomas with *IRF4* breaks ($P=1$), although this analysis was clearly limited by the low number of *KDM4C*-altered cases per group (*Online Supplementary Figure S8*).

Next, we performed differential expression analyses of RNA-sequencing data comparing cases with and without

KDM4C alterations. There were only two morphological subgroups for which sufficient numbers of cases with and without *KDM4C* alterations with RNA-sequencing data were available, namely DLBCL and FL-DLBCL. We performed the differential expression analyses in both of these groups separately. None of the previously described target genes of *KDM4C* (*Online Supplementary Table S3*) was among the 107 differentially expressed genes between *KDM4C* mutated and wildtype cases in the DLBCL group or the 19 differentially expressed genes in the FL-DLBCL group (*Online Supplementary Table S4*). Notably, there appears to be a small but significant difference in gene expression between the *KDM4C*-mutated and *KDM4C*-wildtype cases in the DLBCL group. In contrast, the results in the FL-DLBCL group are in line with common fluctuations that may or may not be due to *KDM4C* status, as this is only one against all other comparisons, and comparing a random FL-DLBCL case against all others often shows even bigger differences. We analyzed the genes differentially expressed between mutated and unmutated *KDM4C* in DLBCL using string-db.⁴⁷ While there are more interactions than randomly expected between the 64 proteins known to string-db (14 vs. 7; $P<0001$), the only enrichment found was in signal peptide domain from UniProt keywords (25 of 64, false discovery rate=0.0135). Next, we intersected the differentially expressed genes based on *KDM4C* mutation status in the DLBCL group with genes differentially expressed between subtypes of DLBCL (ABC, GCB and Type III). However, no significant enrichment in the number of overlapping genes was detected.

Finally, we examined the expression levels of H3 in the cases harboring *KDM4C* aberrations as compared to the cases lacking *KDM4C* alterations, but no significantly differential expression on H3 was detected ($P>0.1$).

Functional analysis of *KDM4C*

We explored public data and screened a total of 23 lymphoma cell lines for the presence of inactivating *KDM4C* alterations using the same approach employed to validate the structural variants described above and combined this with published genomic data from two additional cHL cell lines (*Online Supplementary Table S2*). We detected *KDM4C* deletions in the mycosis fungoides-derived cell line My-La, and the cHL-derived cell line L1236 (*Online Supplementary Table S2*). More specifically, in WGS data of L1236²⁶ we identified a *KDM4C* deletion of approximately 60 kb (chr9: 6,775,810–6,836,328 bp [hg19], comprising exons 2, 3 and 4) at one allele, with an approximately 32 kb internal deletion of the second allele (chr9: 6,795,791–6,828,233 bp [hg19], affecting exons 3 and 4), resulting in homozygous loss of exons 3 and 4 of *KDM4C* (Figure 1B). Whereas the larger heterozygous deletion ablates the canonical translation initiation codon, the 32 kb deletion is predicted to encode an (if translated) non-functional protein in L1236 lacking the N-terminus with the catalytic JmjN domain (Figure 2A). The *KDM4C* heterozygous deletion in My-La cells is in agreement with the conventional cytogenetic analysis describing a del(9)(p21).⁴⁸ In addition, SUP-HD1 and KARPAS-422 cell lines carry the SNV c.G1713A, p.W571*, and c.C2498T, p.P833L, respectively (Figure 2A, *Online Supplementary Table S2*) reported in the COSMIC cell lines database (cancer.sanger.ac.uk/cell_lines), which we validated by PCR and Sanger sequencing and which are predicted as pathogenic variants by FATHMM. Evolutionary and protein structure predictions also suggest that p.P833L is a loss-of-function variant (*Online Supplementary Figure S1*). Thus, remarkably, with L1236 and SUP-HD1 two out of six *bona fide* cHL cell lines show potential inactivating changes in the *KDM4C* gene suggesting a tumor suppressive role in both GC B-cell lymphomas and cHL.

In agreement with the genomic data, *KDM4C* immunoblotting of the various cell lines revealed a complete loss of *KDM4C* protein expression in L1236 cells, and a strong reduction in My-La, but also in the cell lines Se-Ax and SU-DHL-1 using a homemade rabbit polyclonal anti-*KDM4C* antibody (against amino acids 1007–1056) (Figure 2B). To address the functional consequences of *KDM4C* deletions, we constructed an episomally replicating vector for doxycycline-inducible *KDM4C* re-expression in L1236 cells as well as *KDM4C* lentiviruses for re-expression in SU-DHL-1 cells (Figure 2C). In both cell lines, *KDM4C* re-expression resulted in a loss of *KDM4C*-expressing cells over time, in agreement with a tumor suppressor function in these cells. Such an effect was not observed in either KARPAS-422 (p.P833L) or

in NAMALWA (no *KDM4C* aberration) (Figure 2D).

In addition, we aimed to investigate the expression of *KDM4C* by immunohistochemistry in primary tissues as well as cell lines using the anti-*KDM4C* antibody used for the immunoblotting technique. We were able to prove the lack of expression of *KDM4C* protein in L1236 and to specifically detect ectopically expressed *KDM4C* in formalin-fixed and paraffin-embedded transfected HEK293 cells (*data not shown*). However, this as well as several commercially available anti-*KDM4C* antibodies failed in our hands to reliably quantify *KDM4C* protein expression in primary tissues (*data not shown*).

Discussion

Here, we analyzed WGS data of 186 GC B-cell lymphomas to investigate somatic aberrations, including SNV, indels, structural variants, and focal copy number aberrations in 79 genes encoding histone methylation regulators, to identify epigenetic modifiers potentially involved in GC B-cell lymphomagenesis.^{6,11–16} We identified *KDM4C*, encoding a histone demethylase, as being recurrently altered in B-cell lymphomas (7/186, 4%).

Integrating RNA-sequencing and WGS data in the six cases with focal structural variants, we detected alternative *KDM4C* transcripts in five of them. *In silico* analyses using Mechismo predicted that these alternative transcripts result in altered proteins lacking the catalytic or recognition (epigenetic readers) domains, suggesting a loss of function. In contrast, *KDM4C* has been previously described as an oncogene in lymphomas, which is activated by large chromosome 9p gains. These gains mostly derive from co-amplification with *JAK2*, *CD274*, and *PDCD1LG2*, recurrently found in cHL and primary mediastinal B-cell lymphoma.³⁴ Nonetheless, recent studies in these lymphoma subtypes refined the minimally gained region and point to *CD274* and *PDCD1LG2* as main targets, whereas *KDM4C* is not consistently gained (*Online Supplementary Figure S9*). We here detected *KDM4C* to be altered due to focal structural variants (6/7) rather than gross imbalances. Moreover, we observed that the vast majority of focal *KDM4C* aberrations occurred independently of 9p24 amplifications. In brief, *KDM4C* might belong to the increasing list of genes with oncogenic and tumor suppressive function depending on the cellular context and the type of aberration. Examples from hematologic neoplasms include *EZH2* and the CEBP gene family.^{49–51}

In addition to genomic mutations, we explored different other layers that could contribute to dysregulated *KDM4C* in GC B-cell lymphomas. We used previously published data derived from whole genome bisulfite sequencing, array-based DNA methylation, and chromatin state data²²

to investigate epigenetic alterations at the *KDM4C* locus. However, we did not find evidence for epigenetic inactivation of the *KDM4C* locus. Furthermore, we investigated the role of expression of circ*KDM4C*, a circRNA from the *KDM4C* locus recently described to be of pathogenic relevance in solid tumors.^{46,52} Although we detected circ*KDM4C* expression in 1.7% of the cases, none of them showed an alteration of the *KDM4C* locus. Taken together, these results suggest that genomic alterations are the main mechanism involved in *KDM4C* gene dysregulation in GC B-cell lymphomas. The fact that these genomic alterations are mostly focal structural variants and that SNV of *KDM4C* (1/7) seem to be rare in GC B-cell lymphomas likely explains why alterations of this gene have been underestimated in previous whole exome analyses.^{5,6}

KDM4C alterations are not exclusive to GC B-cell NHL. Exploring a set of cell lines we observed that L1236²⁶ and SUP-HD1, and thus two out of six (33.3%) *bona fide* cHL cell lines, show potentially inactivating changes in the *KDM4C* gene, suggesting a tumor suppressive role in both GC B-cell NHL and cHL. We could not detect changes in *KDM4C* transcript expression between cases with altered and wildtype *KDM4C* using RNA-sequencing data of the GC B-cell derived lymphomas in the ICGC cohort. In contrast, using *KDM4C* immunoblotting in the cell lines we observed a complete loss of *KDM4C* protein expression in L1236 cells, and a strong reduction in My-La, which is in line with the genomic analysis. Subsequent functional analyses using *KDM4C* re-expression in cell lines with reduced or lack of *KDM4C* expression support the hypothesis of a tumor suppressor function of *KDM4C* at least in a subset of lymphomas.

In conclusion, our work not only adds *KDM4C* to the list of histone methylation modifiers recurrently altered in B-cell lymphomas, but it also supports a function of *KDM4C* as a tumor suppressor at least in a subset of lymphoma types. Moreover, our data demonstrate that focal structural variants contribute to the mutational burden of distinct genes, which might be missed by pure exome and/or RNA-sequencing approaches. This has to be considered if mutational landscapes are defined for classification schemes, such as those proposed for lymphomas.

Disclosures

No conflicts of interest to disclose.

Contributions

CL performed PCR and Sanger sequencing validations. CL, SB and RSi performed FISH validation analyses. NS, MJ and SM realized the functional analyses. SS, UHT, JS, KK, SHB,

DH, MK, and MS performed analysis of next-generation sequencing data. JMM and RSc developed the *KDM4C* antibody. MG provided the genomic data of cHL cell lines. MS, SH and JOK supervised next-generation sequencing analysis and interpreted data. GA, RBR and JCG generated the protein modeling. AM and WK performed immunohistochemistry analyses. HE, SG, OA, BR and PL analyzed the whole genome bisulfite sequencing and methylation arrays. HLS and MJ provided *KDM4C*-knockout data of cHL cell lines. NS and HLS cloned *KDM4C* expression vectors. RK provided normal B-cell samples. CL, RSi and SM interpreted data and wrote the manuscript. RSi and SM designed the study. RW and CL supported coordination of the project. LT performed the clinical coordination of the project. RSi coordinated the ICGC MMML-Seq network. All authors read and approved the final manuscript.

Acknowledgments

We thank the High Throughput Sequencing Unit of the DKFZ Genomics and Proteomics Core Facility for providing whole-genome sequencing services. We thank Prof. Elias Campo and Blanca González-Farré for support with immunohistochemistry experiments, and Prof. Georg Bornkamm for providing pRTS-1. The support of the technical staff of the Institutes of Human Genetics in Kiel and Ulm, as well as the former masters student, Ivan Potreba, are gratefully acknowledged.

Funding

This study was supported by the German Ministry of Science and Education (BMBF) in the framework of the ICGC MMML-Seq (01KU1002A-J) and ICGC DE-Mining (01KU1505G and 01KU1505E) projects. This work was also supported by the BMBF-funded Heidelberg Center for Human Bioinformatics (HD-HuB) within the German Network for Bioinformatics Infrastructure (de.NBI) (#031A537A, #031A537C). Former grant support for MMML by the Deutsche Krebshilfe (2003-2011) is gratefully acknowledged. CL was supported by an Alexander von Humboldt Foundation post-doctoral fellowship. RSi and MG received funding from the European Union's Horizon 2020 research and innovation program under grant agreement n. 952304. Former support to MG in the form of a FEBS long-term fellowship and a "Support for International Mobility of Scientists" fellowship of the Polish Ministry of Science and Higher Education is gratefully acknowledged.

Data-sharing statement

Sequencing data are available from the European Genome-phenome Archive (EGA) (accession number EGAS00001002199)

References

1. Swerdlow SH, Campo E, Harris NL, Jaffe ES, Pileri SA, Stein H TJ. WHO Classification of Tumours of Haematopoietic and Lymphoid Tissues. 4th ed.; 2017.
2. Rosenwald A, Wright G, Chan WC, et al. The use of molecular profiling to predict survival after chemotherapy for diffuse large-B-cell lymphoma. *N Engl J Med*. 2002;346(25):1937-1947.
3. Hummel M, Bentink S, Berger H, et al. A biologic definition of Burkitt's lymphoma from transcriptional and genomic profiling. *N Engl J Med*. 2006;354(23):2419-2430.
4. Wright GW, Huang DW, Phelan JD, et al. A probabilistic classification tool for genetic subtypes of diffuse large B cell lymphoma with therapeutic implications. *Cancer Cell*. 2020;37(4):551-568.e14.
5. Chapuy B, Stewart C, Dunford AJ, et al. Molecular subtypes of diffuse large B cell lymphoma are associated with distinct pathogenic mechanisms and outcomes. *Nat Med*. 2018;24(5):679-690.
6. Schmitz R, Wright GW, Huang DW, et al. Genetics and pathogenesis of diffuse large B-cell lymphoma. *N Engl J Med*. 2018;378(15):1396-1407.
7. Hübschmann D, Kleinheinz K, Wagener R, et al. Mutational mechanisms shaping the coding and noncoding genome of germinal center derived B-cell lymphomas. *Leukemia*. 2021;35(7):2002-2016.
8. Lacy SE, Barrans SL, Beer PA, et al. Targeted sequencing in DLBCL, molecular subtypes, and outcomes: a Haematological Malignancy Research Network report. *Blood*. 2020;135(20):1759-1771.
9. Runge HFP, Lacy S, Barrans S, et al. Application of the LymphGen classification tool to 928 clinically and genetically-characterised cases of diffuse large B cell lymphoma (DLBCL). *Br J Haematol*. 2021;192(1):216-220.
10. Morin RD, Arthur SE, Hodson DJ. Molecular profiling in diffuse large B-cell lymphoma: why so many types of subtypes? *Br J Haematol*. 2022;196(4):814-829.
11. Pasqualucci L, Dalla-Favera R. Genetics of diffuse large B-cell lymphoma. *Blood*. 2018;131(21):2307-2319.
12. De Silva NS, Klein U. Dynamics of B cells in germinal centres. *Nat Rev Immunol*. 2015;15(3):137-148.
13. Morin RD, Johnson NA, Severson TM, et al. Somatic mutations altering *EZH2* (Tyr641) in follicular and diffuse large B-cell lymphomas of germinal-center origin. *Nat Genet*. 2010;42(2):181-185.
14. Reddy A, Zhang J, Davis NS, et al. Genetic and functional drivers of diffuse large B cell lymphoma. *Cell*. 2017;171(2):481-494.e15.
15. Hashwah H, Schmid CA, Kasser S, et al. Inactivation of CREBBP expands the germinal center B cell compartment, down-regulates MHCII expression and promotes DLBCL growth. *Proc Natl Acad Sci U S A*. 2017;114(36):9701-9706.
16. Krysiak K, Gomez F, White BS, et al. Recurrent somatic mutations affecting B-cell receptor signaling pathway genes in follicular lymphoma. *Blood*. 2017;129(4):473-483.
17. Singleton AB. Exome sequencing: a transformative technology. *Lancet Neurol*. 2011;10(10):942-946.
18. Richter J, Schlesner M, Hoffmann S, et al. Recurrent mutation of the *ID3* gene in Burkitt lymphoma identified by integrated genome, exome and transcriptome sequencing. *Nat Genet*. 2012;44(12):1316-1320.
19. ICGC/TCGA Pan-Cancer Analysis of Whole Genomes Consortium. Pan-cancer analysis of whole genomes. *Nature*. 2020;578(7793):82-93.
20. López C, Kleinheinz K, Aukema SM, et al. Genomic and transcriptomic changes complement each other in the pathogenesis of sporadic Burkitt lymphoma. *Nat Commun*. 2019;10(1):1459.
21. Li H, Kaminski MS, Li Y, et al. Mutations in linker histone genes *HIST1H1 B*, *C*, *D*, and *E*; *OCT2* (*POU2F2*); *IRF8*; and *ARID1A* underlying the pathogenesis of follicular lymphoma. *Blood*. 2014;123(10):1487-1498.
22. Kretzmer H, Bernhart SH, Wang W, et al. DNA methylome analysis in Burkitt and follicular lymphomas identifies differentially methylated regions linked to somatic mutation and transcriptional control. *Nat Genet*. 2015;47(11):1316-1325.
23. Doose G, Haake A, Bernhart SH, et al. *MINCR* is a *MYC*-induced lncRNA able to modulate *MYC*'s transcriptional network in Burkitt lymphoma cells. *Proc Natl Acad Sci U S A*. 2015;112(38):E5261-5270.
24. Otto C, Giefing M, Massow A, et al. Genetic lesions of the *TRAF3* and *MAP3K14* genes in classical Hodgkin lymphoma. *Br J Haematol*. 2012;157(6):702-708.
25. Liu Y, Abdul Razak FR, Terpstra M, et al. The mutational landscape of Hodgkin lymphoma cell lines determined by whole-exome sequencing. *Leukemia*. 2014;28(11):2248-2251.
26. Schneider M, Schneider S, Zühlke-Jenisch R, et al. Alterations of the *CD58* gene in classical Hodgkin lymphoma. *Genes Chromosomes Cancer*. 2015;54(10):638-645.
27. Rausch T, Zichner T, Schlattl A, Stütz AM, Benes V, Korbel JO. *DELLY*: structural variant discovery by integrated paired-end and split-read analysis. *Bioinformatics*. 2012;28(18):i333-i339.
28. Northcott PA, Buchhalter I, Morrissy AS, et al. The whole-genome landscape of medulloblastoma subtypes. *Nature*. 2017;547(7663):311-317.
29. Hoffmann S, Otto C, Kurtz S, et al. Fast mapping of short sequences with mismatches, insertions and deletions using index structures. *PLoS Comput Biol*. 2009;5(9):e1000502.
30. Betts MJ, Lu Q, Jiang Y, et al. Mechismo: predicting the mechanistic impact of mutations and modifications on molecular interactions. *Nucleic Acids Res*. 2015;43(2):e10.
31. Schleussner N, Merkel O, Costanza M, et al. The *AP-1*-*BATF* and *-BATF3* module is essential for growth, survival and *TH17*/*ILC3* skewing of anaplastic large cell lymphoma. *Leukemia*. 2018;32(9):1994-2007.
32. Cloos PAC, Christensen J, Agger K, et al. The putative oncogene *GASC1* demethylates tri- and dimethylated lysine 9 on histone H3. *Nature*. 2006;442(7100):307-311.
33. Loh Y-H, Zhang W, Chen X, George J, Ng H-H. *Jmjd1a* and *Jmjd2c* histone H3 Lys 9 demethylases regulate self-renewal in embryonic stem cells. *Genes Dev*. 2007;21(20):2545-2557.
34. Rui L, Emre NCT, Kruhlik MJ, et al. Cooperative epigenetic modulation by cancer amplicon genes. *Cancer Cell*. 2010;18(6):590-605.
35. Hansen RS, Thomas S, Sandstrom R, et al. Sequencing newly replicated DNA reveals widespread plasticity in human replication timing. *Proc Natl Acad Sci U S A*. 2010;107(1):139-144.
36. Yu K, Huang FT, Lieber MR. DNA substrate length and surrounding sequence affect the activation-induced deaminase activity at cytidine. *J Biol Chem*. 2004;279(8):6496-6500.
37. Krill-Burger JM, Lyons MA, Kelly LA, et al. Renal cell neoplasms contain shared tumor type-specific copy number variations. *Am J Pathol*. 2012;180(6):2427-2439.
38. Lee DH, Kim GW, Jeon YH, Yoo J, Lee SW, Kwon SH. Advances in histone demethylase *KDM4* as cancer therapeutic targets.

- FASEB J. 2020;34(3):3461-3484.
39. Shao N, Cheng J, Huang H, et al. GASC1 promotes hepatocellular carcinoma progression by inhibiting the degradation of ROCK2. *Cell Death Dis.* 2021;12(3):253.
40. Ma X, Ying Y, Sun J, et al. circKDM4C enhances bladder cancer invasion and metastasis through miR-200bc-3p/ZEB1 axis. *Cell Death Discov.* 2021;7(1):365.
41. Chen GQ, Ye P, Ling RS, et al. Histone demethylase KDM4C is required for ovarian cancer stem cell maintenance. *Stem Cells Int.* 2020;2020:8860185.
42. Kleszcz R, Skalski M, Krajka-Kuźniak V, Paluszczak J. The inhibitors of KDM4 and KDM6 histone lysine demethylases enhance the anti-growth effects of erlotinib and HS-173 in head and neck cancer cells. *Eur J Pharm Sci.* 2021;166:105961.
43. Yang D, Xu T, Fan L, Liu K, Li G. microRNA-216b enhances cisplatin-induced apoptosis in osteosarcoma MG63 and SaOS-2 cells by binding to JMJD2C and regulating the HIF1 α /HES1 signaling axis. *J Exp Clin Cancer Res.* 2020;39(1):201.
44. Lang T, Xu J, Zhou L, et al. Disruption of KDM4C-ALDH1A3 feed-forward loop inhibits stemness, tumorigenesis and chemoresistance of gastric cancer stem cells. *Signal Transduct Target Ther.* 2021;6(1):336.
45. Huang Y, Fang J, Bedford MT, Zhang Y, Xu R-M. Recognition of histone H3 lysine-4 methylation by the double tudor domain of JMJD2A. *Science.* 2006;312(5774):748-751.
46. Liang Y, Song X, Li Y, et al. circKDM4C suppresses tumor progression and attenuates doxorubicin resistance by regulating miR-548p/PBLD axis in breast cancer. *Oncogene.* 2019;38(42):6850-6866.
47. Jensen LJ, Kuhn M, Stark M, et al. STRING 8--a global view on proteins and their functional interactions in 630 organisms. *Nucleic Acids Res.* 2009;37(Database issue):D412-416.
48. Netchiporouk E, Gantchev J, Tsang M, et al. Analysis of CTCL cell lines reveals important differences between mycosis fungoides/Sézary syndrome vs. HTLV-1(+) leukemic cell lines. *Oncotarget.* 2017;8(56):95981-95998.
49. Gan L, Yang Y, Li Q, Feng Y, Liu T, Guo W. Epigenetic regulation of cancer progression by EZH2: from biological insights to therapeutic potential. *Biomark Res.* 2018;6(1):10.
50. Tolomeo M, Grimaudo S. The "Janus" role of C/EBPs family members in cancer progression. *Int J Mol Sci.* 2020;21(12):1-18.
51. Shaulian E. AP-1 - the Jun proteins: oncogenes or tumor suppressors in disguise? *Cell Signal.* 2010;22(6):894-899.
52. Ma SD, Xu X, Jones R, et al. PD-1/CTLA-4 blockade inhibits Epstein-Barr virus-induced lymphoma growth in a cord blood humanized-mouse model. *PLoS Pathog.* 2016;12(5):e1005642.